Li *et al. BMC Plant Biol* (2021) 21:326
https://doi.org/10.1186/s12870-021-03112-4

BMC Plant Biology

RESEARCH ARTICLE Open Access

Glycolate oxidase-dependent H_2O_2 production regulates IAA biosynthesis in rice

Xiangyang Li[1,2], Mengmeng Liao[1,2], Jiayu Huang[1,2], Zheng Xu[1,2], Zhanqiao Lin[1,2], Nenghui Ye[3], Zhisheng Zhang[1,2*] and Xinxiang Peng[1,2]

Abstract

Background: Glycolate oxidase (GLO) is not only a key enzyme in photorespiration but also a major engine for H_2O_2 production in plants. Catalase (CAT)-dependent H_2O_2 decomposition has been previously reported to be involved in the regulation of IAA biosynthesis. However, it is still not known which mechanism contributed to the H_2O_2 production in IAA regulation.

Results: In this study, we found that in *glo* mutants of rice, as H_2O_2 levels decreased IAA contents significantly increased, whereas high CO_2 abolished the difference in H_2O_2 and IAA contents between *glo* mutants and WT. Further analyses showed that tryptophan (Trp, the precursor for IAA biosynthesis in the Trp-dependent biosynthetic pathway) also accumulated due to increased tryptophan synthetase β (TSB) activity. Moreover, expression of the genes involved in Trp-dependent IAA biosynthesis and IBA to IAA conversion were correspondingly up-regulated, further implicating that both pathways contribute to IAA biosynthesis as mediated by the GLO-dependent production of H_2O_2.

Conclusion: We investigated the function of GLO in IAA signaling in different levels from transcription, enzyme activities to metabolic levels. The results suggest that GLO-dependent H_2O_2 signaling, essentially via photorespiration, confers regulation over IAA biosynthesis in rice plants.

Keywords: Glycolate oxidase, H_2O_2, IAA, Photorespiration, Rice

Background

Photorespiration is the second-highest metabolic flux after photosynthesis in plants. It starts from the synthesis of 2-phosphoglycolate (2-PG) catalyzed by the oxygenase activity of ribulose-1,5-bisphosphate carboxylase/oxygenase (RuBisCO). 2-PG is immediately converted to glycolate in chloroplasts and transported to peroxisomes, where glycolate is detoxified into glycine by the glycolate/glyoxylate/glycine metabolic steps [1]. Glycolate oxidase (GLO, EC 1.1.3.15) is a key enzyme for the glycolate-glyoxylate conversion during photorespiration, which catalyzes the oxidation of glycolate to generate glyoxylate and H_2O_2 [2]. It has been estimated that the photorespiratory H_2O_2 produced by GLO may account for approximately 70% of the total H_2O_2 in C3 plants, thus making an important contribution to cellular redox status and participating in multiple H_2O_2-related processes [2]. GLO activity was reported to be up-regulated in pea, cowpea, and tobacco under drought stress [3–5]. More importantly, GLO-derived H_2O_2 can mediate non-host resistance and gene-for-gene-mediated resistance in *Arabidopsis thaliana* and *Nicotiana benthamiana* [6], and it is also involved in *barley stripe mosaic virus* infection in barley and basal defense against *Pseudomonas syringae* in tomato [7, 8]. In addition, initiation of the systemic acquired acclimation and formation of iron plaques on the surface of roots in plants is mediated by GLO-derived H_2O_2 [9, 10].

*Correspondence: zzsheng@scau.edu.cn
[1] State Key Laboratory for Conservation and Utilization of Subtropical Agro-Bioresources, College of Life Sciences, South China Agricultural University, No.483, Wushan Road, 510642 Guangzhou, China
Full list of author information is available at the end of the article

H_2O_2, as a typical reactive oxygen species, is not only biologically toxic but also serves as an important signaling molecule. Its homeostasis is elaborately regulated by the balance between the cellular generation and scavenging rates [11]. Photorespiratory H_2O_2 is mainly scavenged by peroxisomal catalase (CAT, EC 1.11.1.6), and GLO and CAT usually act in concert to regulate intracellular photorespiratory H_2O_2 levels in plants [11]. It has been observed that CAT-dependent H_2O_2 cross-talks with other phytohormone signaling pathways. For instance, ABA regulates the expression of peroxisomal CAT and hence the levels of H_2O_2 in water-stressed *Arabidopsis* [12]. Another potential point of crosstalk is between the CAT-dependent H_2O_2 and IAA signaling pathway, which has recently gained much attention. Gao et al. [13] found that the absence of the photorespiratory CAT2 resulted in accumulation of the photorespiratory H_2O_2. Additionally, increased H_2O_2 suppressed the IAA synthesis in *Arabidopsis*. In turn, exogenous auxin activated IAA signaling to counteract photorespiratory H_2O_2-dependent cell death in *Arabidopsis cat2* mutants [14]. Yuan et al. [15] further demonstrated that the accumulated H_2O_2 in *Arabidopsis* resulting from CAT2 inhibition promoted the sulfenic acid modification of tryptophan synthetase β (TSB) subunit 1, subsequently decreasing TSB activity to repress the synthesis of the IAA precursor Trp. While CAT-dependent H_2O_2 decomposition intertwined with the IAA signaling pathway, the molecular details of this process remain scarce, and more notably, it is not clear whether GLO dependent H_2O_2 production plays a major role in IAA regulation.

As an important engine for H_2O_2 production, GLO has various isoforms that are encoded by multi-gene families in plants. *AtGOX1* and *AtGOX2* are the major isoforms involved in basic photorespiration metabolism in *Arabidopsis thaliana* [6]. We have earlier demonstrated that *OsGLO1* and *OsGLO4* are the dominant isoforms for photorespiration in rice [16, 17]. In this study, in order to understand whether and how GLO-dependent H_2O_2 modulates IAA signaling, various genetically-modified rice lines of *GLO1* and *GLO4* were generated. It was found that IAA levels in *glo1* and *glo4* knockout mutants were significantly up-regulated which was correlated with lower peroxisomal H_2O_2 levels. Further analyses showed that IAA and Trp contents were increased, and that TSB activity and the genes related to Trp-dependent IAA biosynthesis and IBA to IAA conversion were also up-regulated. The results suggest that GLO-dependent H_2O_2 production can regulate IAA biosynthesis in rice.

Results

Rice GLO mutants exhibited photorespiration phenotypes as accompanied with decreased peroxisomal H_2O_2

The rice genome contains four *GLO* homologs, i.e., *GLO1* (Os03g0786100), *GLO3* (Os04g0623500), *GLO4* (Os07g0152900), and *GLO5* (Os07g0616500). *GLO1* and *GLO4* are the primary *GLO* genes that contribute to photorespiratory glycolate-glyoxylate metabolism [16, 17]. In this study, knockout and overexpression lines of *GLO1* and *GLO4* were generated in rice. Western blot analysis confirmed that GLO1 and GLO4 were absent in the *glo1* and *glo4* knockout mutants, respectively (Additional file 1A, B). GLO activities were decreased by approximately 55% and 30% in the *glo1* and *glo4* mutants, respectively. In *GLO* overexpression (*GLO*OE) lines, GLO activities were increased by 60–95% in *GLO1*OE lines and 40–55% in *GLO4*OE lines (Fig. 1A and Additional file 2A). Both seedlings of *glo1* and *glo4* knockout mutants showed dwarfish growth as compared with WT but recovered to normal stature when photorespiration was suppressed under high CO_2 condition (Fig. 1B, C and D). The growth phenotypes of those overexpression lines have been described earlier in our previous study. Briefly, the growth of *GLO*OE lines was improved when GLO activities were increased by 60–100%, whereas reduced growth was noticed when GLO activity was increased over 150% [18]. In addition, some downstream enzymes of GLO, such as SGAT and GGAT, were little altered in all GLO modified lines under both ambient and high CO_2 conditions (Fig. 2 and Additional file 2). The CAT activity was suppressed by 30 to 40% under high CO_2, but there was no difference in CAT activities between various GLO modified lines under ambient and high CO_2 conditions (Fig. 2A and Additional file 2B). This is consistent with previous studies showing that GLO downstream steps in photorespiration are not significantly affected by GLO modification [19–21].

As the fastest pathway for H_2O_2 production, photorespiratory H_2O_2 is mainly generated by the GLO-catalyzed glycolate oxidation reaction [1, 2]. The absence of *GLO1* and *GLO4* can significantly decrease H_2O_2 levels in rice leaves under atmospheric condition (Fig. 3A, B), and this difference disappeared under high CO_2 (Fig. 3B). No significant changes were observed in *GLO1* and *GLO4* overexpression lines under both atmospheric and high CO_2 conditions (Additional file 3A, B). To further prove that the decreased H_2O_2 levels occur in peroxisomes, we quantified the transcript abundance of two previously identified peroxisome-specific H_2O_2-responsive genes, *OsbHLH168* (Os01g0108600) and *OsSAP17* (Os09g0385700) [22, 23], by qRT-PCR. As shown in Fig. 3C, transcript levels of both *OsbHLH168* and *OsSAP17* were significantly lowered in the *glo1* and *glo4*

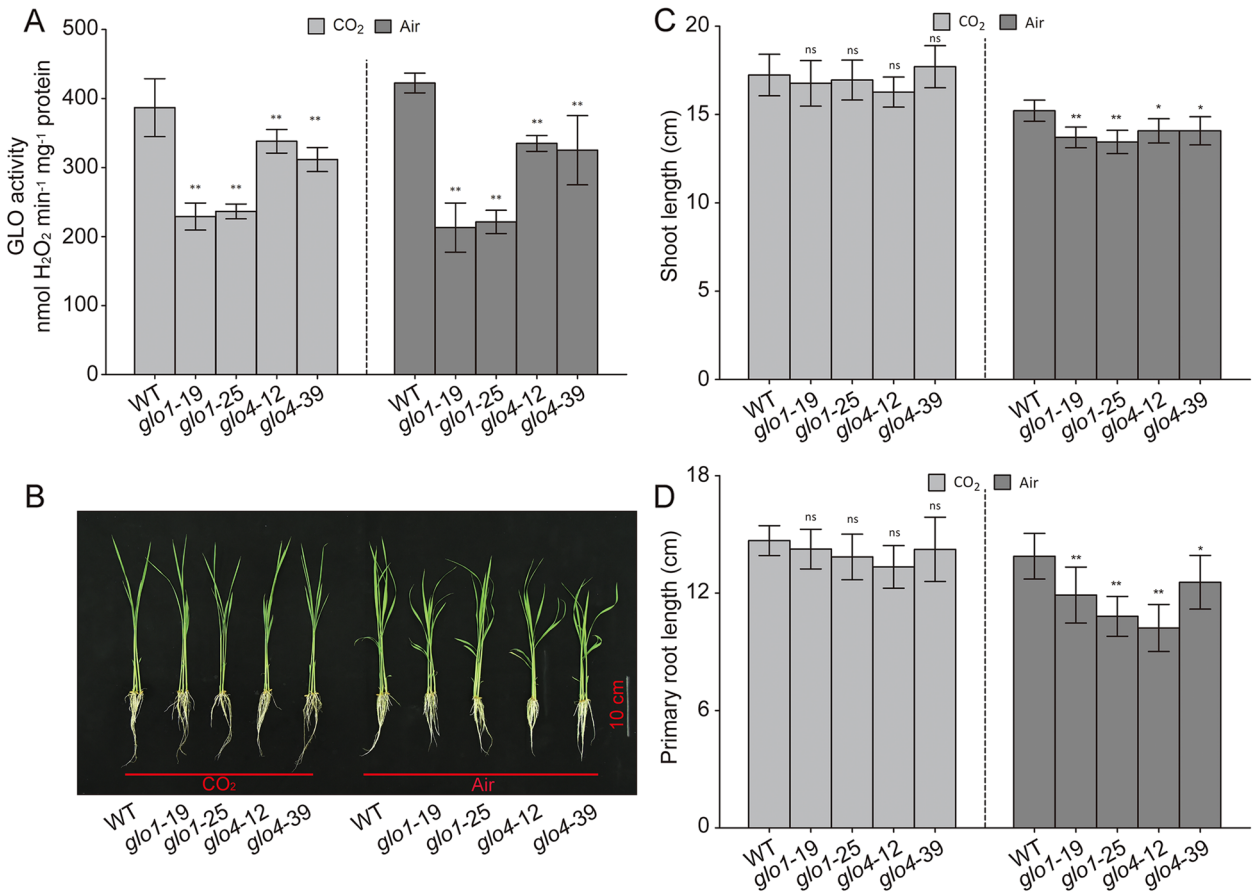

Fig. 1 GLO activity and growth phenotype of *glo1* and *glo4* mutants. Germinated seeds of *glo1* and *glo4* mutants were divided into two groups and cultured in two growth chambers under atmospheric and high CO_2 (3500 ppm) conditions. The seedlings were then used for GLO activity measurement (**A**), phenotypic photo (**B**), shoot length and primary root length statistics (**C**, **D**). Results are representative of three independent experiments. Data are presented as means ± SD of three biological replications, $^{*}P < 0.05$, $^{**}P < 0.01$ according to Student's *t*-tests

mutants under atmospheric condition. For *GLO* overexpression lines, the expression levels of these two genes were not significantly different (Additional file 3C). These results indicated that the decreased H_2O_2 levels occurred in peroxisomes, due to reduced GLO activities in *glo1* and *glo4* mutants.

The GLO-dependent H_2O_2 production regulated IAA and Trp levels

It was previously reported that the CAT-dependent H_2O_2 accumulation can suppress IAA synthesis in *Arabidopsis* [13, 15]. Since CAT and GLO may work cooperatively [11], it is of interest to further understand whether GLO is involved in the H_2O_2-IAA crosstalk. As the peroxisomal H_2O_2 levels were decreased (Fig. 3), the IAA contents were increased by 25–30% and 15–20% in the *glo1* and *glo4* knockout mutants, respectively (Fig. 4A). No obvious changes in IAA were observed in overexpression lines (Additional file 4A), in which H_2O_2 levels were unchanged (Additional file 3). Trp is the primary precursor for IAA biosynthesis in plants [24, 25], so we further determined if Trp contents were affected in various *GLO* genetically-modified rice lines. As shown in Fig. 4B, Trp content was about 6.5 μg g^{-1} FW in WT, which was increased to 8.5–10.0 μg g^{-1} FW in *glo1* knockout mutants, and 8.0–8.5 μg g^{-1} FW in *glo4* knockout mutants. No obvious changes were detected in the overexpression lines (Additional file 4B). Also, Trp contents were changed with a similar tendency as IAA. When GLO-dependent H_2O_2 production was suppressed under high CO_2 condition, the differences in IAA and Trp contents in *glo1* and *glo4* knockout mutants vanished (Fig. 4A, B). The above results indicated that the reduced photorespiratory H_2O_2 resulting from the reduction of GLO activity was correlated with increased IAA and Trp contents in rice.

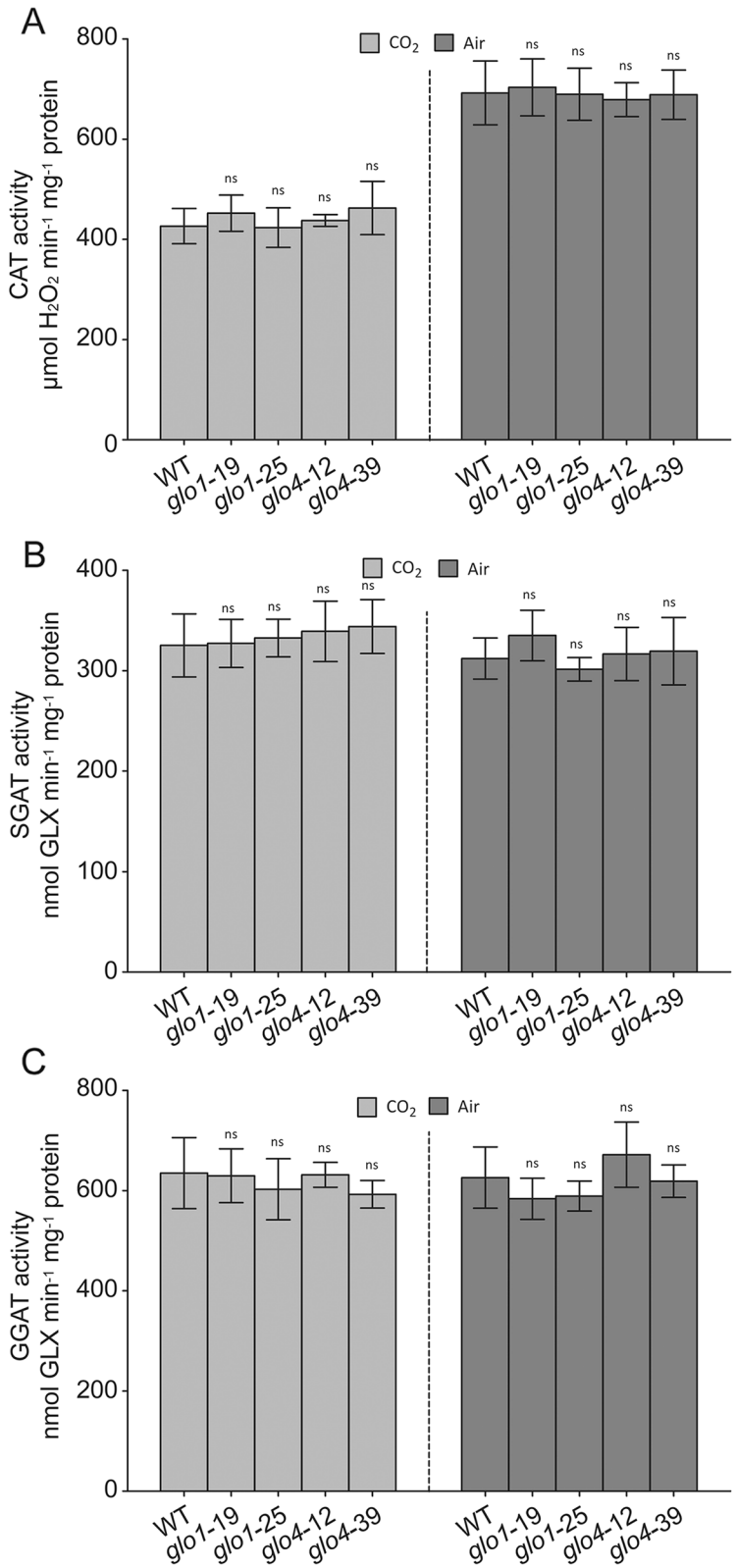

Fig. 2 The activity of CAT, SGAT and GGAT in *glo1* and *glo4* mutants. Germinated seeds of *glo1* and *glo4* mutants were cultured under atmospheric and high CO_2 (3500 ppm) conditions. The seedlings were then used for CAT (**A**), SGAT (**B**) and GGAT (**C**) activity measurement. Data are presented as means ± SD of three biological replications, $*p < 0.05$, $**p < 0.01$ according to Student's *t*-test

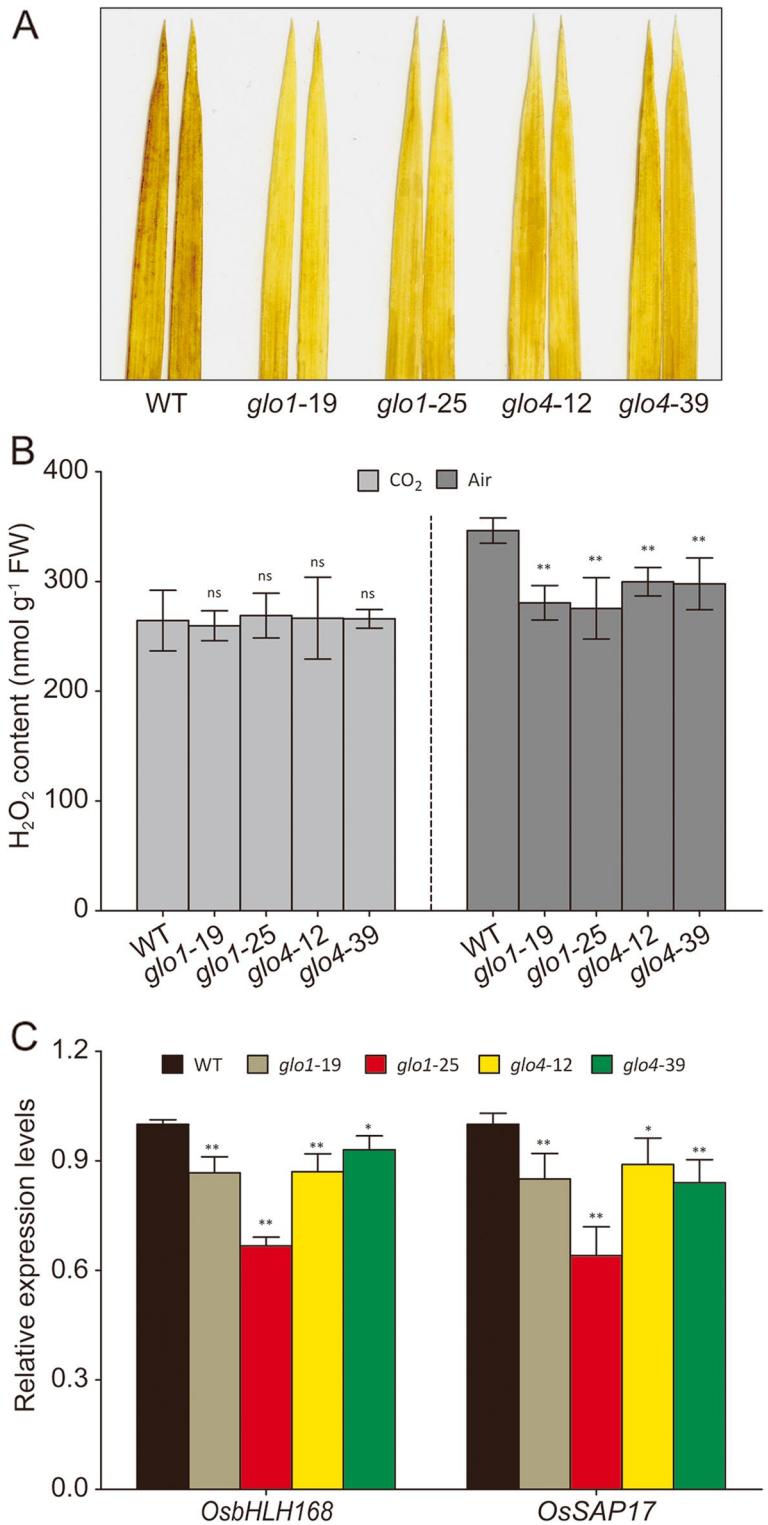

Fig. 3 Detection of H_2O_2 levels in *glo1* and *glo4* mutants. H_2O_2-DAB staining of rice leaves under atmospheric condition (**A**); endogenous H_2O_2 contents of rice leaves under atmospheric and high CO_2 condition (**B**); qRT-PCR analysis of peroxisomal H_2O_2-responsive genes in *glo1* and *glo4* mutants under atmospheric condition (**C**), the two H_2O_2 indicators selected were previously identified peroxisome-specific H_2O_2-responsive genes, *OsbHLH168* (Os01g0108600) and *OsSAP17* (Os09g0385700). Results are representative of three independent experiments. Data are presented as means ± SD of three biological replications, $^*P < 0.05$, $^{**}P < 0.01$ according to Student's *t*-tests

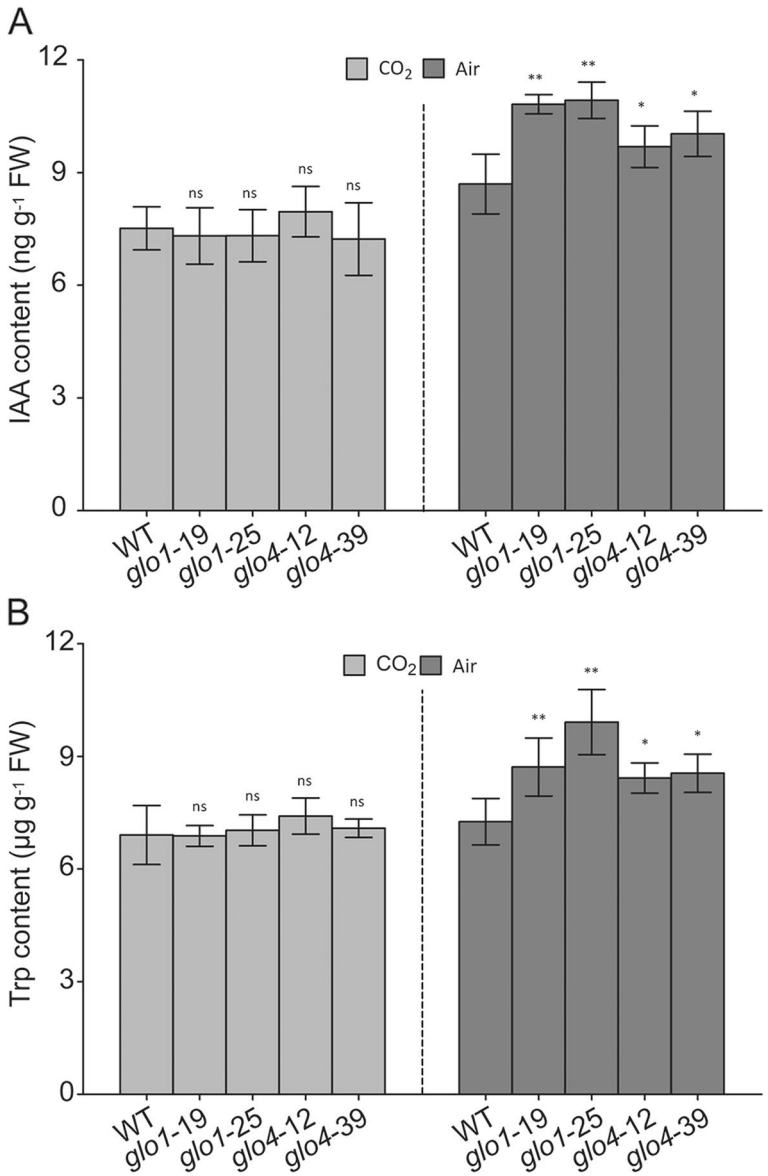

Fig. 4 Changes of IAA and Trp levels in *glo1* and *glo4* mutants. Germinated seeds were cultured under atmospheric and high CO_2 conditions. The leaves of five-leaf stage rice seedlings were then detached for determining IAA (**A**) and Trp (**B**). Data are presented as means ± SD of three biological replications, $^{*}P < 0.05$, $^{**}P < 0.01$ according to Student's *t*-tests

The regulation of IAA occurred at the biosynthetic level

Theoretically, IAA content may be regulated at the levels of biosynthesis and sequestration [26]. The Trp-dependent pathway has been known to dominate IAA biosynthesis, so we first detected TSB activities that are responsible for the biosynthesis of the IAA precursor Trp. As shown in Fig. 5A, TSB activities were increased by 40% and 27% in *glo1* and *glo4* mutants, respectively. No changes were observed in *GLO* overexpression lines (Additional file 5). Correspondingly, transcripts of the two subunits of tryptophan synthase (β subunit 1, *TSB1*; α subunit 1, *TSA1*) were also significantly enhanced in *glo* mutants (Fig. 5B). Besides, some other downstream genes involved in the Trp-dependent IAA biosynthesis (Additional file 6), i.e. *OsYUC2* (Os01g0732700), *OsYUC5* (Os07g0437000), *OsAO3* (Os03g0790700), and *OsAMI1* (Os04g0118100), were still up-regulated in *glo* mutants (Fig. 5B).

The conversion of IBA to IAA occurr in the peroxisome, which could be intimately regulated by the redox state of peroxisomes [27, 28]. Hence, the expressions levels of those genes proposed to be involved in the conversion of IBA to IAA were determined (Additional file 6),

i.e. *OsIBR3* (Os07g0675133), *OsECH2* (Os09g0544900), and *OsIBR1* (Os09g0133200). These data showed that all of these genes were up-regulated in *glo* mutants (Fig. 5C).

Finally, the expression levels of various IAA-responsive/transport genes, which are known to be regulated in an IAA-dependent manner, were analyzed (Additional file 7). As expected, the genes involved in IAA responsive and transport processes, i.e. *OsAIL5* (Os04g0653600), *OsAIL7* (Os03g0313100), *OsPBP1* (Os01g0783700), *OsIAA26* (Os09g0527700), and *OsLAZY1* (Os11g0490600), *OsNS3* (Os10g0147400), *OsNS4* (Os11g0169200) were transcriptionally up-regulated in *glo* mutants (Fig. 6A, B), and these genes may further function in multiple plant growth processes and stress responses. The above results collectively indicate that the GLO-dependent H_2O_2 production regulates IAA biosynthesis to perform various biological functions in rice.

Discussion

In recent decades, information has become increasingly available indicating that photorespiration can influence various biological processes, e.g., carbon metabolism, energetics, nitrogen assimilation, and respiration [29–31]. Remarkably, photorespiration is a major source for H_2O_2 in photoautotrophic tissues, thereby making important contributions to cellular redox status and signaling [2, 11, 30]. Reports indicate that H_2O_2 is closely associated with IAA during plant development, and that IAA can facilitate H_2O_2 accumulation in the roots of maize, tomato, and *Arabidopsis* to regulate root growth and gravitropism [32–34], while IAA biosynthesis and signaling were inhibited by both exogenous and endogenous H_2O_2 in *Arabidopsis* seedlings [35, 36]. Nevertheless, how H_2O_2 production and signaling interact with IAA is still not well understood. Gao et al. [13] demonstrated that the CAT-dependent H_2O_2 was involved in the regulation of IAA, but no direct evidence was provided as to whether the H_2O_2 is derived from photorespiration, because CAT-dependent H_2O_2 may come from other sources in the peroxisome, such as fatty acid β-oxidation and dismutation of $O_2^{\cdot-}$ [37]. By using *GLO* knockout mutants, we further demonstrated that the GLO-dependent H_2O_2 also regulated IAA levels in rice (Fig. 3 and Fig. 4A). However, overexpression of either *GLO1* or *GLO4* conferred no significant changes in H_2O_2 levels (Additional file 3), or on IAA contents (Additional file 4A). It has been similarly noticed that overexpression of GLO conferred no enhanced effects on photorespiratory flux and H_2O_2 production, considering that several photorespiratory enzymes (e.g. GLO, 2-phosphoglycolate phosphatase) are sufficiently high to manage the metabolic flux of photorespiration under normal conditions [18, 38] and further up-regulation is only beneficial under some stress environments [3–5, 8]. Overall, our present results suggest that GLO-dependent H_2O_2 regulates IAA levels in rice, not only supporting the results from the *Arabidopsis cat2* mutants [13, 14], but also providing direct evidence that the CAT-dependent H_2O_2 ultimately comes from the GLO-catalyzed reaction, essentially via photorespiratory metabolism in plants.

Two IAA biosynthetic strategies exist in plants, namely, Trp-independent and Trp-dependent pathways. Indole-3-glycerol phosphate and indole are the likely precursors of Trp-independent IAA biosynthesis, but its complete biochemical pathway has not yet been elucidated. Trp is the precursor in the Trp-dependent IAA biosynthesis, and several pathways have been proposed for the IAA biosynthetic strategy, but molecular and genetic evidence of the key enzymes involved in such pathways are still not confirmed [24, 25]. Tryptophan synthetase β (TSB), which catalyzes Trp formation from Ser and indole, is a key limiting factor in Trp biosynthesis. It has also been documented that elevated H_2O_2 content in *Arabidopsis* leaves decreased TSB activity, thus reducing Trp and IAA levels [15, 39]. Our present study showed that the increased TSB activity (Fig. 5A) and up-regulated expression of genes responsible for the Trp-dependent IAA biosynthesis (Fig. 5B) were positively correlated with the increased levels of Trp and IAA in *glo* mutants (Fig. 4A, B). These lines of evidence suggest that the Trp-dependent pathway may have dominated in the IAA biosynthesis of rice plants that is regulated by GLO-dependent H_2O_2. In addition, modifications in IAA can alter its activity and sequester active IAA [40]. For example, IBA is a chain-elongated form of IAA and functions as a pool for sequestering IAA, which may still be an efficient mechanism for IAA regulation in plants once IBA is converted to IAA [27, 40, 41]. Altering the pool of IAA derived from IBA is known to result in a set of developmental defects in *Arabidopsis* [42, 43]. IBA is likely converted to IAA through a β-oxidation pathway in the peroxisome [27, 40], where H_2O_2 might serve as a key regulator [28]. Although we failed to accurately determine IBA contents

(See figure on next page.)

Fig. 5 TSB activity and expression patterns of IAA synthesis-related genes in *glo1 and glo4* mutants. (**A**) TSB activity in *glo* mutants. **(B)** Expression patterns of genes participating in Trp biosynthesis and Trp-dependent IAA biosynthesis**.** (**C**) Expression patterns of genes involved in the conversion of IBA to IAA. The leaves of five-leaf stage rice seedlings grown in atmospheric condition were detached for TSB activity measurement and RNA extraction. Data are presented as means ± SD of three biological replications, $^*P < 0.05$, $^{**}P < 0.01$ according to Student's *t*-tests

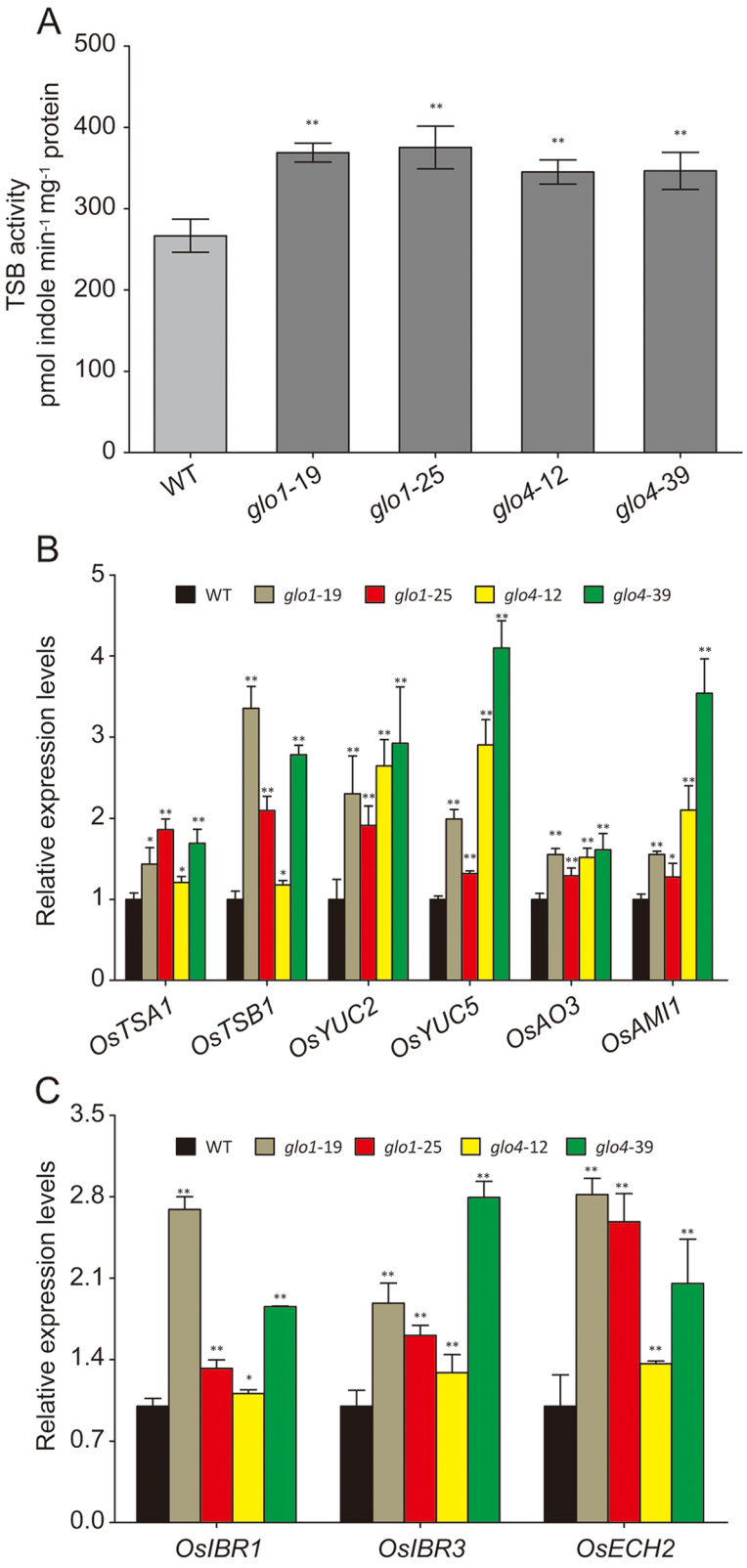

Fig. 5 (See legend on previous page.)

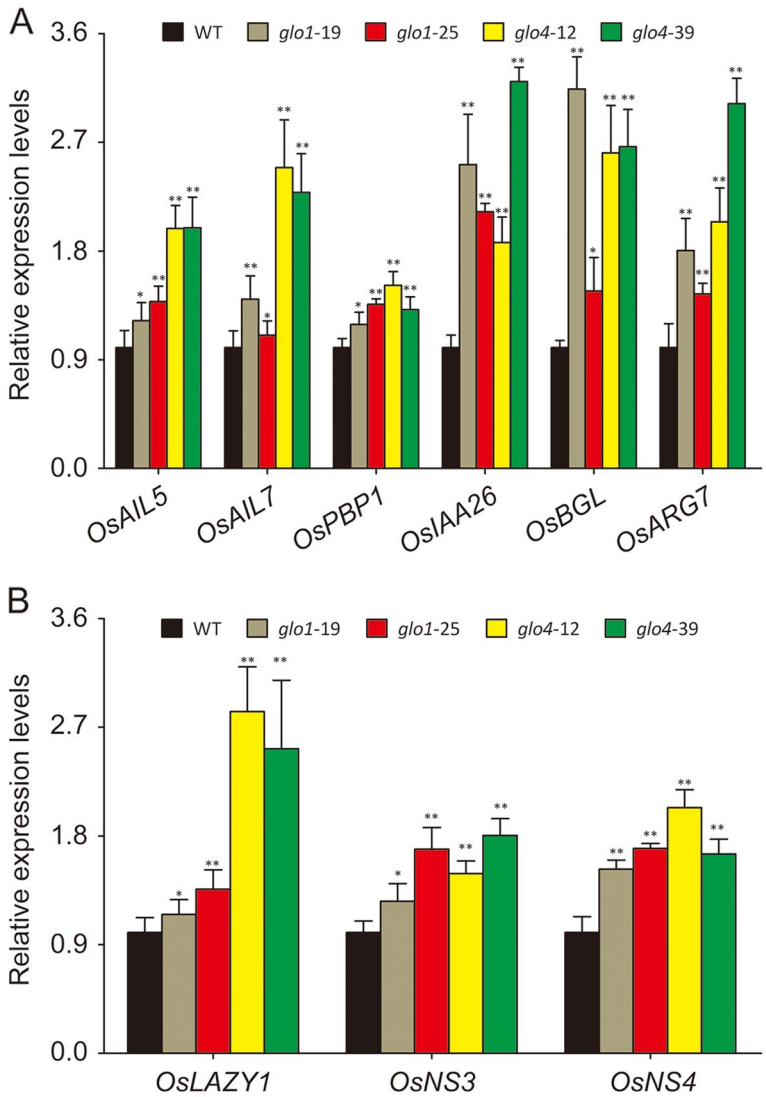

Fig. 6 Expression patterns of IAA responsive/transport genes in *glo1* and *glo4* mutants. (**A**) Expression patterns of genes in response to IAA content. (**B**) Expression patterns of genes involved in IAA transport. The leaves of five-leaf stage rice seedlings grown in atmospheric condition were detached for RNA extraction. Data are means ± SD of three biological replications, $^{*}P < 0.05$, $^{**}P < 0.01$ according to Student's *t*-tests

due to technical difficulties [27, 44], the expression levels of the genes involved in the IBA to IAA conversion were shown to be significantly up-regulated in the *glo* mutants (Fig. 5C). Therefore, it is likely that the elevated IAA levels caused by decreased H_2O_2 levels in *glo* mutants may partially be contributed by the increased conversion of IBA to IAA.

It is well known that IAA signaling controls numerous plant growth and development processes by regulating the expression of various IAA response factors/genes. Indeed, the expression of many IAA-responsive/transport genes (Additional file 7) was markedly up-regulated in *glo1* and *glo4* mutants (Fig. 6A, B). Our current data, in combination with the results from other studies [13, 15], strongly support that IAA levels can be regulated by either CAT or GLO in plants. IAA is a key phytohormone responding to various environmental stresses, and growth inhibition by decreased IAA levels is an important physiological strategy for plants in response to drought and pathogen infection [45, 46]. Meanwhile, GLO can be induced by drought, high temperature and pathogen infection [3, 5, 8], and these stresses can also result in salicylic acid (SA) accumulation in plants [47–49]. We have previously proposed a switch model, in which a physical association-dissociation of GLO and CAT, in response to stimuli such as SA, serves as a mechanism to modulate cellular H_2O_2 levels [11]. More interestingly, it has been documented that SA could negatively

regulate the synthesis and/or signaling of IAA, they act in a mutually antagonistic manner in plants [50–53], and a recent study further suggested that SA regulation of IAA is mediated by H_2O_2 [15]. Therefore, we speculate that SA may modulate H_2O_2 through our proposed switch model, subsequently conferring regulation on IAA. Moreover, the regulation of H_2O_2 may occur in a fluctuating manner because the association-dissociation of GLO and CAT could take place dynamically and transiently in response to environmental stresses or stimuli, e.g., drought and pathogen infection. Therefore, we here further modified our proposed model, in which the switch-modulated H_2O_2 fluctuation confers biological functions via regulating IAA levels in plants (Fig. 7).

Conclusion

In this study, we found that decreases in GLO-dependent H_2O_2 levels were accompanied with IAA and Trp accumulation in *glo* rice mutants, whereas high CO_2 was able to abolish the IAA difference. Subsequent analyses of transcript levels and enzyme activities of genes involved in IAA metabolism suggest that both Trp-dependent IAA biosynthesis and IBA to IAA conversion contribute to the increase of IAA contents. This data offer insights into how GLO-dependent H_2O_2, essentially via photorespiration, regulates IAA biosynthesis in plants. Furthermore, taken together with our previously reported association-dissociation mechanism of GLO and CAT, we further consider that H_2O_2 waves as regulated by SA via such a proposed mechanism may be an important point for crosstalk between SA and IAA. However, molecular details of this signalling pathway and its biological significance remain an important issue for our future research.

Methods

Plant materials, growth conditions, and treatments

Oryza sativa cv. Zhonghua 11 (japonica cultivar-group) preserved by our laboratory was used for the functional analyses and *GLO* transgenic line construction [20]. Pre-germinated rice seeds were grown in Kimura B complete nutrient solution under natural conditions. After reaching the four-leaf stage, seedlings were transplanted, either being continuously grown in Kimura B complete nutrient solution in a plant growth chamber with a light cycle of 14 h light/10 h dark (30 °C / 25 °C, respectively) at 600 μmol photons m^{-2} s^{-1} on average, relative humidity 60%-80%, or grown in paddy fields under natural conditions. For high concentration CO_2 treatment, pre-germinated rice seeds were cultured in Kimura B complete nutrient solution in a plant growth chamber (Percival E-41HO, USA) supplied with 3500 ppm CO_2 [30, 54, 55].

Generation of genetically modified rice lines

Total RNA was extracted using the Plant RNA Purification Reagent (Magen Biotech), cDNA was prepared from 1 μg of total RNA using HiScript® II Reverse Transcriptase (Vazyme) as recommended. To generate *GLO* overexpression transgenic lines, each *GLO* sequence was cloned into the pYLox.5 vector using the ClonExpress Ultra One Step Cloning Kit (Vazyme) [56]. For the generation of CRISPR-Cas9 knockout lines, specific targeting sequences of *GLO1* and *GLO4* (Additional file 8) were synthesized and cloned into the pYLCRISPR/Cas9Pubi vector [57]. The constructed vectors were transformed into rice callus using *Agrobacterium*-mediated infection (strain *EHA105*). The T1 seeds from the positive T0 lines were germinated and then transplanted into soil to grow until the T2 seeds were harvested. After that, the T2 homozygous plants that originated from two independent lines were used for subsequent treatments and analyses.

Enzyme assays and protein measurement

GLO activity assay

GLO activity was detected in an enzyme coupled assay [16]. Briefly, 0.1 g leaves were detached from the youngest fully expanded leaves (five-leaf stage) and homogenized in 1 mL of 50 mM PBS (pH 7.4) at 4 °C, the homogenates were centrifuged at 12 000 g for 20 min at 4 °C and the supernatants were used as enzyme extracts. The 1 mL reaction mixture containing 50 mM PBS (pH 7.8), 1 mM 4-amino-antipyrine, 0.1 mM FMN, 2 mM phenol, 5 units of horseradish peroxidase, and 5 mM glycolate. The reaction was started by adding enzyme and the absorbance at 520 nm was recorded at intervals of 5 s for 1 min. The protein content was determined using Coomassie brilliant blue G250.

TSB activity assay

TSB activity was measured according to Last et al. [39]. All steps were performed at 4 °C, unless indicated otherwise. Plant extracts were prepared by grinding 1 g of leaves from five-leaf stage rice seedlings into a paste with a prechilled mortar and pestle containing 1.5 mL of 0.1 M K-phosphate (pH 8.2), 0.3 g quartz sand, and 0.1 g polyvinylpolypyrrolidone. Homogenates were then centrifuged twice at 12,000 g for 15 min and the supernatants were used as the enzyme extracts. The 1 mL reaction solution was prepared containing 60 mM L-serine, 0.2 mM indole, 80 mM potassium phosphate (pH8.2), 10 μg pyridoxal phosphate, and 0.4 mL plant extract with gentle agitation at 30 °C. The reaction was stopped by the addition of 0.1 mL of 0.2 M sodium hydroxide after 90 min. The

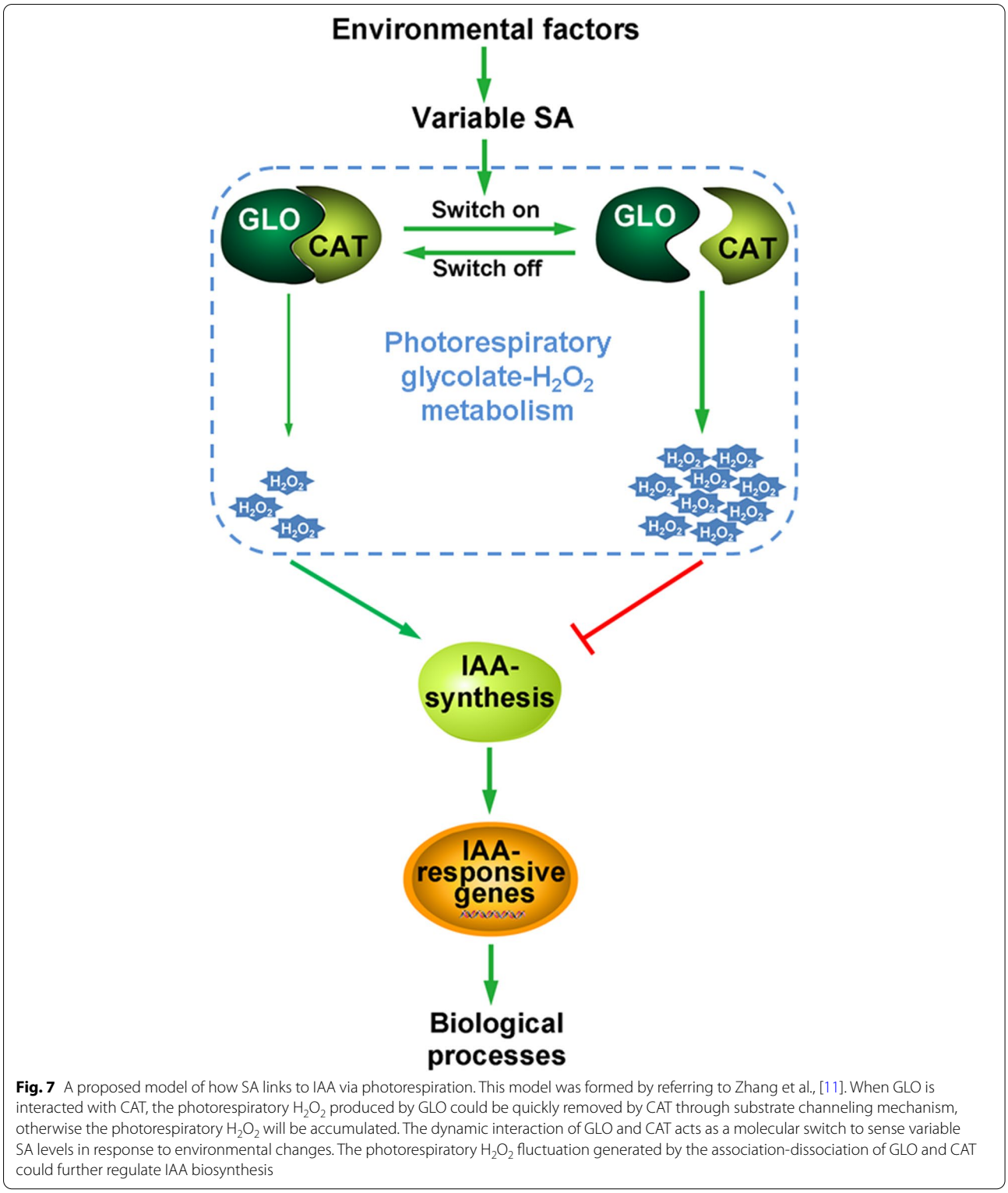

Fig. 7 A proposed model of how SA links to IAA via photorespiration. This model was formed by referring to Zhang et al., [11]. When GLO is interacted with CAT, the photorespiratory H_2O_2 produced by GLO could be quickly removed by CAT through substrate channeling mechanism, otherwise the photorespiratory H_2O_2 will be accumulated. The dynamic interaction of GLO and CAT acts as a molecular switch to sense variable SA levels in response to environmental changes. The photorespiratory H_2O_2 fluctuation generated by the association-dissociation of GLO and CAT could further regulate IAA biosynthesis

residual indole was extracted into 4 mL of toluene by gentle vortexing (vigorous agitation created a permanent emulsion). After centrifugation for 15 min at 1500 g, 0.5 mL of the toluene layer was added to 2 mL ethanol and 1 mL Ehrlich's Reagent (Sigma). The color could develop for 30 min at room temperature and the absorbance of the product was measured spectrophotometrically at 540 nm.

SGAT and GGAT activities assay

SGAT and GGAT activities were measured by detecting the reduction of glyoxylate according to Yu et al. [58] with some modifications. Briefly, 50 mg of leaves (five-leaf stage) were homogenized in 1 mL 50 mM K-phosphate (pH 7.4) at 4℃, and the homogenate was then centrifuged at 12 000 g and 4℃ for 15 min. The supernatant was used as enzyme extract. The 0.5 mL enzymatic reaction mixture containing 50 mM K-phosphate (pH7.4), 50 mM glyoxylate, 5.5 mM pyridoxal-5-phosphate and appropriate enzyme extract. The enzymatic reaction was started by adding 20 mM L-serine for SGAT or 20 mM L-glutamate for GGAT at 30℃ for 20 min. This enzymatic reaction was terminated by adding 0.1 mL 2 M HCl and neutralized with 0.1 mL 2 M NaOH. After that, 0.1 mL 0.33% phenylhydrazine hydrochloride was added to the mixture and incubated at 30℃ for 15 min. Finally, 0.5 mL HCl and 0.1 mL 1.65% potassium ferricyanide was added for color reaction, the red color produced was measured at 520 nm.

CAT activity assay

The CAT activity was detected using a UV spectrophotometer in a reaction mixture containing 50 mM PBS (pH 7.4), 25 mM H_2O_2 at 30℃. The consumption of H_2O_2 was measured at 240 nm and the CAT activity was calculated using the extinction coefficient for H_2O_2 of 43.6 M^{-1} cm^{-1} [11].

3, 3′-diaminobenzidine (DAB) staining for H_2O_2 detection

The leaf H_2O_2 abundance was determined in situ by DAB uptake methods [11]. The youngest fully expanded leaves (10 cm, at the five-leaf stage) were detached, and the cut end was dipped into DAB solution (1 mg ml^{-1}, pH 3.8) for 2 h in a growth chamber (light intensity 700 μmol m^{-2} s^{-1}, temperature 25 °C, and relative humidity 60%). After that, the leaves were de-stained twice with ethanol and photographed.

Assay of H_2O_2 content

Endogenous H_2O_2 content in rice leaves (at five-leaf stage) were measured using an Amplex Red H_2O_2/peroxidase assay kit (Invitrogen, USA) [11]. Briefly, 0.1 g leaves were detached and immediately ground in liquid nitrogen, and then the powder was extracted in 1 ml PBS (50 mM, pH 7.4) and centrifuged at 12 000 g for 15 min at 4℃. The supernatant was used to determine H_2O_2 levels.

Quantification of IAA

For IAA quantification, 1 g of leave material was detached from the youngest fully expanded leaves (five-leaf stage) and immediately frozen in liquid nitrogen. The extraction and quantification of endogenous IAA were conducted according to the manufacturer's instructions (Wuhan Metware Biotechnology Co., Ltd., Wuhan, China) [59]. Briefly, 50 mg of frozen leaf material was ground into a powder and extracted with methanol/water/formic acid (15:4:1, V/V/V). The combined extracts were evaporated to dryness under a stream of nitrogen gas, were reconstituted in 80% methanol (V/V), and filtered (PTFE, 0.22 μm, Anpel) before LC–MS/MS analysis. The quantification of IAA was conducted using an ultra-performance liquid chromatography-tandem mass spectrometry (LC–MS/MS) system (UPLC, Shim-pack UFLC SHIMADZU CBM30A system, Kyoto, Japan; MS, Applied Biosystems, Foster City, CA). The content of IAA was determined using an external standard method and was expressed as ng/g fresh weight (FW). Three biological replications were performed per sample.

Determination of Trp content

Measurement of Trp content was based on a method reported previously with some modifications [60]. The youngest fully expanded leaves were detached and frozen in liquid nitrogen immediately for subsequent analysis. Harvested leaves were sampled at 0.5 g each and homogenized in 3 mL of 2% (w/v) sulphosalicylic acid. After incubating at 25 °C for 2 h, the homogenates were centrifuged at 12 000 g for 20 min, and then the supernatants were filtered through a 0.22 μm nylon membrane. Trp contents in the filtrates were determined with a high-speed automatic amino acid analyzer (Hitachi 835–50, Tokyo, Japan).

Real-time quantitative PCR (qRT-PCR) analysis

The total RNA and cDNA were prepared as described above. To quantify the expression levels of genes related to peroxisomal H_2O_2 production and IAA metabolism in leaves of various *GLO* transgenic rice lines and WT, qRT-PCR analysis was performed on a Bio-Rad CFX96 apparatus with SYBR Green I dye (Vazyme). PCR was carried out in 96-well plates using the following program: denaturation for 5 min at 95 °C, followed by 40 cycles of denaturation for 10 s at 95 °C and incorporative annealing and extension for 30 s at 60 °C. The primers used for qRT-PCR were designed on a dedicated website (https://biodb.swu.edu.cn/qprimerdb/?tds-ourcetag=s_pcqq_aiomsg). The data were normalized to the amplification of the *OsActin1* gene (Os03g0718100). All experiments were performed with three biological and three technical replicates per biological replicate. The primer sequences used in this paper are presented in Supporting Information (Additional files 9, 10).

Abbreviations
GLO: Glycolate oxidase; CAT: Catalase; IBA: Indole-3-butyric acid; IAA: Indole-3-acetic acid; TSB: Tryptophan synthetase β; qRT-PCR: Real-time quantitative PCR.

Supplementary Information

The online version contains supplementary material available at https://doi.org/10.1186/s12870-021-03112-4.

Additional file 1.
Additional file 2.
Additional file 3.
Additional file 4.
Additional file 5.
Additional file 6.
Additional file 7.
Additional file 8.
Additional file 9.
Additional file 10.

Acknowledgements
The authors would like to thank Prof. Yao-Guang Liu (College of Life Sciences, South China Agricultural University) for providing the pYLox.5 and pYLCRISPR/Cas9 vectors.

Authors' contributions
ZZS designed the experiments. LXY, LMM, HJY, XZ and LZQ performed most of experiments and analyzed the data. YNH assisted in experiments. ZZS and PXX wrote the manuscript. All authors read and approved the final manuscript.

Funding
This work was supported by the Major Program of Guangdong Basic and Applied Research (2019B030302006), the National Natural Science Foundation of China (32070265, 31770256), and the Natural Science Foundation of Guangdong Province (2019A1515011438). The funding bodies had no role in the design of this study and collection, analysis, and interpretation of data and in writing the manuscript.

Availability of data and materials
All data generated or analyzed during this study are included in this published article and its supplementary information files; the datasets and accession numbers used during the current study (Os03g0786100, Os04g0623500, Os07g0152900, Os07g0616500, Os01g0108600, Os09g0385700, Os01g0732700, Os07g0437000, Os03g0790700, Os04g0118100, Os07g0675133, Os09g0544900, Os09g0133200, Os04g0653600, Os03g0313100, Os01g0783700, Os09g0527700, Os11g0490600, Os10g0147400, Os11g0169200, Os03g0718100) are available in the Rice Annotation Project (RAP) repository (https://rapdb.dna.affrc.go.jp/index.html).

Declarations

Ethics approval and consent to participate
Not applicable.

Consent to publication
Not applicable.

Competing interests
The authors declare that they have no competing interests.

Author details
[1]State Key Laboratory for Conservation and Utilization of Subtropical Agro-Bioresources, College of Life Sciences, South China Agricultural University, No.483, Wushan Road, 510642 Guangzhou, China. [2]Guangdong Laboratory for Lingnan Modern Agricultural Science and Technology, South China Agricultural University, No.483, Wushan Road, Guangzhou 510642, China. [3]College of Agronomy, Hunan Agricultural University, No.1, Nongda Road, Changsha 410128, China.

Received: 28 September 2020 Accepted: 28 June 2021
Published online: 06 July 2021

References

1. Dellero Y, Jossier M, Schmitz J, Maurino VG, Hodges M. Photorespiratory glycolate-glyoxylate metabolism. J Exp Bot. 2016;67(10):3041–52.
2. Noctor G, Veljoviv-Jovanovic S, Driscoll S, Novitskaya L, Foyer CH. Drought and Oxidative Load in the Leaves of C3 Plants: a Predominant Role for Photorespiration? Ann Bot. 2002;89(7):841–50.
3. Rizhsky L, Liang H, Mittler R. The combined effect of drought stress and heat shock on gene expression in tobacco. Plant Physiol. 2002;130(3):1143–51.
4. Mittler R, Zilinskas BA. Regulation of pea cytosolic ascorbate peroxidase and other antioxidant enzymes during the progression of drought stress and following recovery from drought. Plant J. 1994;5(3):397–405.
5. Mukherjee SP, Choudhuri MA. Implications of water stress-induced changes in the levels of endogenous ascorbic acid and hydrogen peroxide in *Vigna* seedlings. Physiol Plantarum. 1983;58(2):166–70.
6. Rojas CM, Senthil-Kumar M, Wang K, Ryu C, Kaundal A, Mysore KS. Glycolate Oxidase Modulates Reactive Oxygen Species-Mediated Signal Transduction during Nonhost Resistance in *Nicotiana benthamiana* and *Arabidopsis*. Plant Cell. 2012;24(1):336–52.
7. Yang M, Li Z, Zhang K, Zhang X, Zhang Y, Wang X, Han C, Yu J, Xu K, Li D. *Barley Stripe Mosaic Virus* γb Interacts with Glycolate Oxidase and Inhibits Peroxisomal ROS Production to Facilitate Virus Infection. Mol Plant. 2018;11:338–41.
8. Ahammed GJ, Li X, Zhang G, Zhang H, Shi J, Pan C, Yu J, Shi K. Tomato photorespiratory glycolate-oxidase-derived H_2O_2 production contributes to basal defence against *Pseudomonas syringae*. Plant Cell Environ. 2018;41(5):1126–38.
9. Yu X, Wu D, Fu Y, Yang X, Baluška F, Shen H. OsGLO4 is involved in the formation of iron plaques on surface of rice roots grown under alternative wetting and drying condition. Plant Soil. 2018;423(1):111–23.
10. Xia X, Zhou Y, Shi K, Zhou J, Foyer CH, Yu J. Interplay between reactive oxygen species and hormones in the control of plant development and stress tolerance. J Exp Bot. 2015;66(10):2839–56.
11. Zhang Z, Xu Y, Xie Z, Li X, He Z, Peng X. Association-Dissociation of Glycolate Oxidase with Catalase in Rice: A Potential Switch to Modulate Intracellular H_2O_2 Levels. Mol Plant. 2016;9(5):737–48.
12. Ye N, Zhu G, Liu Y, Li Y, Zhang J. ABA Controls H_2O_2 Accumulation Through the Induction of OsCATB in Rice Leaves Under Water Stress. Plant Cell Physiol. 2011;52(4):689–98.
13. Gao X, Hong MY, Hu YQ, Li J, Lu Y. Mutation of *Arabidopsis* CATALASE2 results in hyponastic leaves by changes of auxin levels. Plant Cell Environ. 2014;37(1):175–88.
14. Kerchev P, Mühlenbock P, Denecker J, Morreel K, Hoeberichts FA, Van Der Kelen K, Vandorpe M, Nguyen L, Audenaert D, Van Breusegem F. Activation of auxin signalling counteracts photorespiratory H_2O_2-dependent cell death. Plant Cell Environ. 2015;38(2):253–65.
15. Yuan H, Liu W, Lu Y. CATALASE2 Coordinates SA-Mediated Repression of Both Auxin Accumulation and JA Biosynthesis in Plant Defenses. Cell Host Microbe. 2017;21(2):143–55.
16. Zhang Z, Li X, Cui L, Meng S, Ye N, Peng X. Catalytic and functional aspects of different isozymes of glycolate oxidase in rice. BMC Plant Biol. 2017;17(1):110–35.
17. Zhang Z, Lu Y, Zhai L, Deng R, Jiang J, Li Y, He Z, Peng X. Glycolate Oxidase Isozymes Are Coordinately Controlled by GLO1 and GLO4 in Rice. Plos One. 2012; 7(6): e39658.

18. Cui L, Lu Y, Li Y, Yang C, Peng X. Overexpression of Glycolate Oxidase Confers Improved Photosynthesis under High Light and High Temperature in Rice. Front Plant Sci. 2016;7:1165.
19. Zelitch I, Schultes NP, Peterson RB, Brown P, Brutnell TP. High Glycolate Oxidase Activity Is Required for Survival of Maize in Normal Air. Plant Physiol. 2009;149(1):195–204.
20. Xu H, Zhang J, Zeng J, Jiang L, Liu E. Inducible antisense suppression of glycolate oxidase reveals its strong regulation over photosynthesis in rice. J Exp Bot. 2009;60(6):1799–809.
21. Lu Y, Li Y, Yang Q, Zhang Z, Chen Y, Zhang S, Peng X. Suppression of glycolate oxidase causes glyoxylate accumulation that inhibits photosynthesis through deactivating Rubisco in rice. Physiol Plantarum. 2014;150(3):463–76.
22. Sewelam N, Jaspert N, Van Der Kelen K, Tognetti VB, Schmitz J, Frerigmann H, Stahl E, Zeier J, Van Breusegem F, Maurino VG. Spatial H_2O_2 Signaling Specificity: H_2O_2 from Chloroplasts and Peroxisomes Modulates the Plant Transcriptome Differentially. Mol Plant. 2014;7(7):1191–210.
23. Tyagi H, Jha S, Sharma M, Giri J, Tyagi AK. Rice SAPs are responsive to multiple biotic stresses and overexpression of OsSAP1, an A20/AN1 zinc-finger protein, enhances the basal resistance against pathogen infection in tobacco. Plant Sci. 2014;225:68–76.
24. Di D, Zhang C, Luo P, An C, Guo G. The biosynthesis of auxin: how many paths truly lead to IAA? Plant Growth Regul. 2016;78(3):275–85.
25. Mano Y, Nemoto K. The pathway of auxin biosynthesis in plants. J Exp Bot. 2012;63(8):2853–72.
26. Spiess GM, Zolman BK. Peroxisomes as a source of auxin signaling molecules. Subcell Biochem. 2013;69:257–81.
27. Frick EM, Strader LC. Roles for IBA-derived auxin in plant development. J Exp Bot. 2018;69(2):169–77.
28. Tognetti VB, Van Aken O, Morreel K, Vandenbroucke K, van de Cotte B, De Clercq I, Chiwocha S, Fenske R, Prinsen E, Boerjan W, et al. Perturbation of indole-3-butyric acid homeostasis by the UDP-glucosyltransferase UGT74E2 modulates *Arabidopsis* architecture and water stress tolerance. Plant Cell. 2010;22(8):2660–79.
29. Fernie AR, Bauwe H. Wasteful, essential, evolutionary stepping stone? The multiple personalities of the photorespiratory pathway. Plant J. 2020;102(4):666–77.
30. Foyer CH, Noctor G. Redox Homeostasis and Signaling in a Higher-CO_2 World. Annu Rev Plant Biol. 2020;71:157–82.
31. Florian A, Timm S, Nikoloski Z, Tohge T, Bauwe H, Araujo WL, Fernie AR. Analysis of metabolic alterations in *Arabidopsis* following changes in the carbon dioxide and oxygen partial pressures. J Intger Plant Biol. 2014;56(9):941–59.
32. Ivanchenko MG, den Os D, Monshausen GB, Dubrovsky JG, Bednářová A, Krishnan N. Auxin increases the hydrogen peroxide (H_2O_2) concentration in tomato (*Solanum lycopersicum*) root tips while inhibiting root growth. Ann Bot. 2013;112(6):1107–16.
33. Peer WA, Cheng Y, Murphy AS. Evidence of oxidative attenuation of auxin signalling. J Exp Bot. 2013;64(9):2629–39.
34. Joo JH, Bae YS, Lee JS. Role of Auxin-Induced Reactive Oxygen Species in Root Gravitropism. Plant Physiol. 2001;126(3):1055–60.
35. Jia N, Lv TT, Li MX, Wei SS, Li YY, Zhao CL, Li B. The J-protein AtDjB1 is required for mitochondrial complex I activity and regulates growth and development through ROS-mediated auxin signalling. J Exp Bot. 2016;67(11):3481–96.
36. Wang PC, Du YY, An GY, Zhou Y, Miao C, Song CP. Analysis of Global Expression Profiles of *Arabidopsis* Genes Under Abscisic Acid and H_2O_2 Applications. J Intger Plant Biol. 2006;48(1):62–74.
37. Sandalio L, Rodríguez-Serrano M, Romero-Puertas M, Del Río L. Role of peroxisomes as a source of reactive oxygen species (ROS) signaling molecules. Subcell Biochem. 2012;69:231–55.
38. Timm S, Hagemann M. Photorespiration-how is it regulated and how does it regulate overall plant metabolism? J Exp Bot. 2020;71(14):3955–65.
39. Last RL, Bissinger PH, Mahoney DJ, Radwanski ER, Fink GR. Tryptophan mutants in *Arabidopsis*: the consequences of duplicated tryptophan synthase beta genes. Plant Cell. 1991;3(4):345–58.
40. Woodward AW, Bartel B. Auxin: regulation, action, and interaction. Ann Bot. 2005;95(5):707–35.
41. Korasick DA, Enders TA, Strader LC. Auxin biosynthesis and storage forms. J Exp Bot. 2013;64(9):2541–55.
42. Strader LC, Bartel B. Transport and Metabolism of the Endogenous Auxin Precursor Indole-3-Butyric Acid. Mol Plant. 2011;4(3):477–86.
43. Strader LC, Culler AH, Cohen JD, Bartel B. Conversion of Endogenous Indole-3-Butyric Acid to Indole-3-Acetic Acid Drives Cell Expansion in *Arabidopsis* Seedlings. Plant Physiol. 2010;153(4):1577–86.
44. Novak O, Henykova E, Sairanen I, Kowalczyk M, Pospisil T, Ljung K. Tissue-specific profiling of the *Arabidopsis thaliana* auxin metabolome. Plant J. 2012;72(3):523–36.
45. Shi H, Chen L, Ye T, Liu X, Ding K, Chan Z. Modulation of auxin content in *Arabidopsis* confers improved drought stress resistance. Plant Physiol Biochem. 2014;82:209–17.
46. Fu J, Wang S. Insights into auxin signaling in plant-pathogen interactions. Front Plant Sci. 2011;2:74.
47. Yang L, Li B, Zheng X, Li J, Yang M, Dong X, He G, An C, Deng XW. Salicylic acid biosynthesis is enhanced and contributes to increased biotrophic pathogen resistance in *Arabidopsis* hybrids. Nat Commun. 2015;6:7309.
48. Okuma E, Nozawa R, Murata Y, Miura K. Accumulation of endogenous salicylic acid confers drought tolerance to *Arabidopsis*. Plant Signal Behav. 2014; 9(3):e28085.
49. Hara M, Furukawa J, Sato A, Mizoguchi T, Miura K. Abiotic Stress and Role of Salicylic Acid in Plants. In: Abiotic Stress Responses in Plants: Metabolism, Productivity and Sustainability. Edited by Ahmad P, Prasad MNV. New York: Springer New York; 2012; 235–251.
50. Iglesias MJ, Terrile MC, Casalongué CA. Auxin and salicylic acid signalings counteract the regulation of adaptive responses to stress. Plant Signal Behav. 2011;6(3):452–4.
51. Kazan K, Manners JM. Linking development to defense: auxin in plant-pathogen interactions. Trends Plant Sci. 2009;14(7):373–82.
52. Wang D, Pajerowska-Mukhtar K, Culler AH, Dong X. Salicylic acid inhibits pathogen growth in plants through repression of the auxin signaling pathway. Curr Biol. 2007;17(20):1784–90.
53. Vlot AC, Dempsey DA, Klessig DF. Salicylic Acid, a multifaceted hormone to combat disease. Annu Rev Phytopathol. 2009;47:177–206.
54. Wingler A, Lea PJ, Quick WP, Leegood RC. Photorespiration: metabolic pathways and their role in stress protection. Phil Trans R Soc Lond B. 2000;355(1402):1517–29.
55. Cui L, Zhang C, Li Z, Xian T, Wang L, Zhang Z, Zhu G, Peng X. Two chloroplastic PLGG1 isoforms function together to transport photorespiratory glycolate and glycerate in rice. J Exp Bot. 2021; erab020. doi: https://doi.org/10.1093/jxb/erab020.
56. Zhang Z, Liang X, Lu L, Xu Z, Huang J, He H, Peng X. Two glyoxylate reductase isoforms are functionally redundant but required under high photorespiration conditions in rice. BMC Plant Biol. 2020;20(1):1–12.
57. Ma X, Zhang Q, Zhu Q, Wei L, Yan C, Rong Q, Wang B, Yang Z, Li H, Lin Y. A robust CRISPR/Cas9 system for convenient, high-efficiency multiplex genome editing in monocot and dicot plants. Mol Plant. 2015;8(8):1274–84.
58. Yu L, Jiang J, Zhang C, Jiang L, Ye N, Lu Y, Yang G, Liu E, Peng C, He Z, Peng X. Glyoxylate rather than ascorbate is an efficient precursor for oxalate biosynthesis in rice. J Exp Bot. 2010;61(6):1625–34.
59. He Y, Zhao J, Yang B, Sun S, Peng L, Wang Z. Indole-3-acetate beta-glucosyltransferase OsIAGLU regulates seed vigour through mediating crosstalk between auxin and abscisic acid in rice. Plant Biotechnol J. 2020;18(9):1933–45.
60. Masclaux-Daubresse C. Glutamine Synthetase-Glutamate Synthase Pathway and Glutamate Dehydrogenase Play Distinct Roles in the Sink-Source Nitrogen Cycle in Tobacco. Plant Physiol. 2006;140(2):444–56.

Publisher's Note